MARINE & MARITIME INTELLIGENT ROBOTICS

UNIVERSITÉ DE TOULON

Modeling and control Underwater Vehicle: Sparus

Abdelhaleem SAAD, Yosef GUEVARA.

Underwater Robotics, Modelling and Control

January 15, 2023

Contents

1 Introduction

The purpose of this report is to understand the theory behind an accurate mathematical model estimation of and AUV. By calculating the elements for rigid body dynamics for a 6 DOF underwater vehicle, such the system inertia matrix, the damping equation and posterior simulation, given by the equation.

$$M\dot{v} + C(v)v + g(\eta) + g_o = \tau \tag{1}$$

where

- M = Inertia Matrix(including added mass).
- $C(v)$ = Matrix of Coreolis Centripetal term (Including added mass).
- $D(v)$ = Damping matrix.
- $g(\eta)$ = Vector of gravitational forces and moments.
- τ = Vector of control inputs.

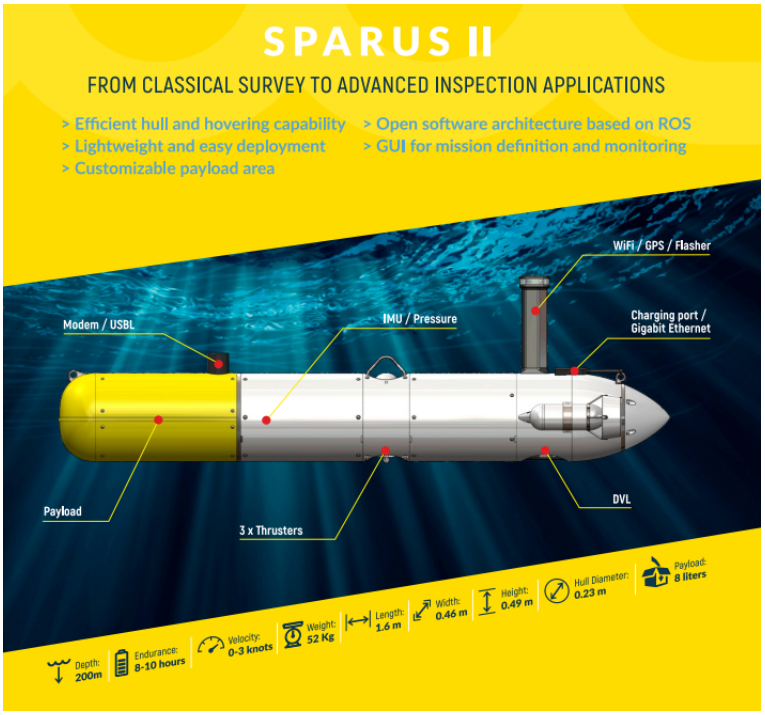

Figure 1: Sparus II technical overview.

The Sparus II AUV is a lightweight autonomous underwater vehicle for a maximum depth of 200 m from the Spanish company IQUA robotics. Given its torpedo-shape, it is capable of hovering and has an easily configurable payload area and an open software architecture, making it a multipurpose platform.

The main objective of this project is to calculate the mass matrices of each element of the Sparrus, as well as the calculation of the added mass matrices, drag matrices, and the impact on the coefficients of the global mass matrix when simulating imposed linear accelerations and constant linear velocities.

2 The Sparus Autonomous Vehicle

2.1 Vehicle specifications

The dimensional specification of the vehicle are given by:

Technical specifications	
Specification	Description
Length	1.6 m
Hull diameter	0.23m
Mass	No 52 Kg
Buoyancy mass	No 52.1 kg

Table 1: Technical specifications

The values of the sensors and thrusters positions for the Sparus are:

Sensor and Thruster positions		
	Coordinates in basse b	Values in m
Motor 1	$\vec{r}_{t1}^{b} = (d_{1x}, d_{1y}, d_{1z})^T$	$(0,\ 0,\ 0.08)$
Motor 2	$\vec{r}_{t2}^{b} = (d_{2x}, d_{2y}, d_{2z})^T$	$(-0.59, 0.17, 0)$
Motor 3	$\vec{r}_{t3}^{b} = (d_{3x}, d_{3y}, d_{3z})^T$	$(-0.59, -0.17, 0)$
DVL	$\vec{r}_{t3}^{b} = (d_{dx}, d_{dy}, d_{dz})^T$	$(-0.4145, 0, 0.11)$
IMU and Depth	$\vec{r}_{t3}^{b} = (d_{ix}, d_{iy}, d_{iz})^T$	$(0.364, -0.021, -0.085)$
USBL	$\vec{r}_{t3}^{b} = (d_{ux}, d_{uy}, d_{uz})^T$	$(0.44, 0, -0.14)$

Table 2: Sensor and Thruster positions

2.2 Vehicle geometry

To obtain a close approximation to the real vehicle, a series of simplifications and assumptions of the model were made. The model shape was simplified, as can be seen in the comparison images.

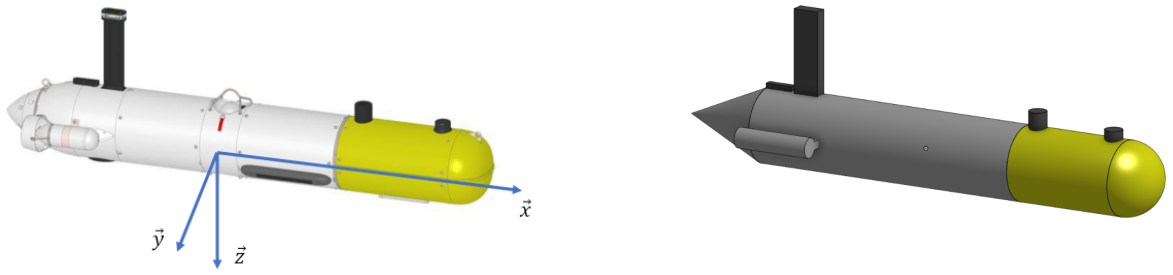

(a) Sparus II UV original CAD model (b) Sparus II UV simplified CAD model

Figure 2: Sparus II 3D models

The simplified model dimensions, are the following ones.

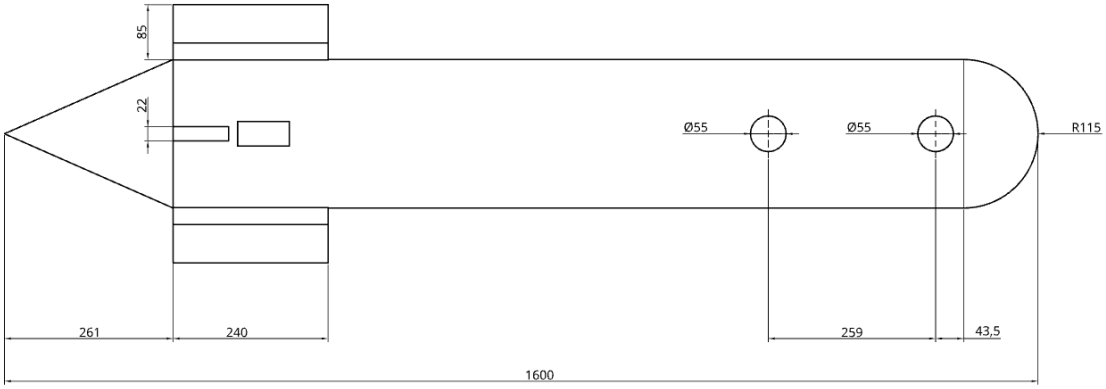

Figure 3: Sparus II simplified model top view.

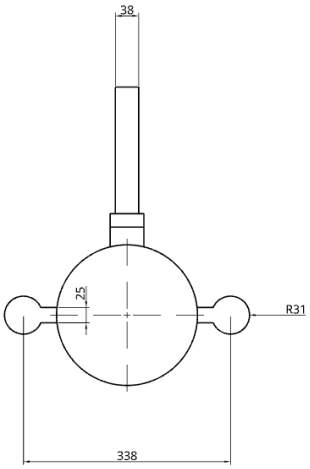

Figure 4: Sparus II simplified model front view.

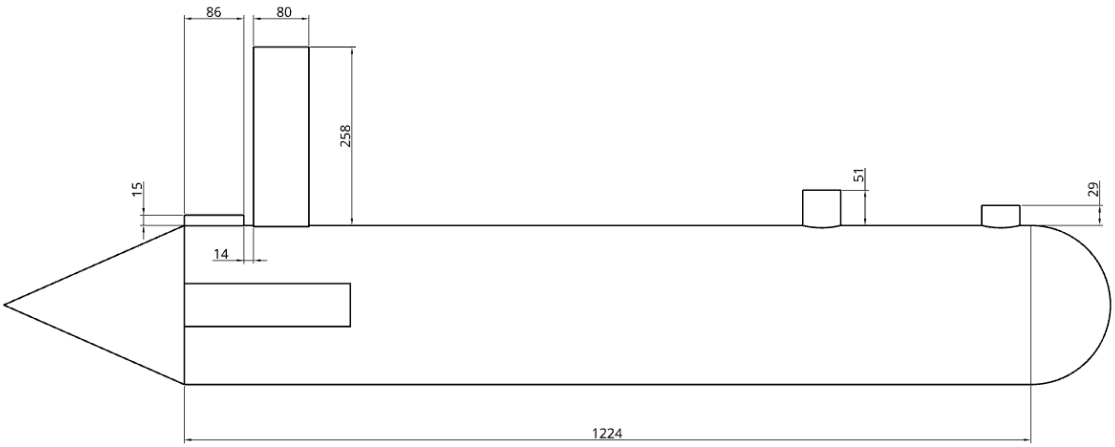

Figure 5: Sparus II simplified model lateral view.

It is obvious that this vehicle is XY-axis and YZ-axis symmetrical.

3 Mass Matrix computation

The mass matrix represents the distribution of mass in a rigid body. The diagonal elements of the matrix represent the mass of the body in each degree of freedom, meanwhile, the cross-coupling effects between the DOF, such as the interaction between translation and rotation. This matrix plays a fundamental role in the equations that define the movement of the vehicle, allowing us to calculate the accelerations of a given system given the forces and torques acting on it, making it a crucial factor in the dynamics of the system.

If we consider the density of the vehicle as constant, we can use the CAD simplified model to calculate the vehicle's approximate volume and density.

$$Density = \frac{Mass}{Volume} \tag{2}$$

$$Density = \frac{52\ Kg}{0.06\ m^3} = 866.67\ Kg/m^{-3}$$

In other hand, The Sparus allows defining the main axes and the position of the gravity center. Therefore, we consider the origin of the base **body** in the gravity center of the Sparus. It is placed at the x-position of the central thruster and at the middle of the cylinder.

$$M_{RB} = \begin{bmatrix} mI_{3\times3} & -mS(r_g^b) \\ mS(r_g^b) & I_b \end{bmatrix} = \begin{bmatrix} m & 0 & 0 & 0 & mz_g & -my_g \\ 0 & m & 0 & -mz_g & 0 & -mx_g \\ 0 & 0 & m & my_g & -mx_g & 0 \\ 0 & -mz_g & my_g & I_x & -I_{xy} & -I_{xz} \\ mz_g & 0 & -mx_g & -I_{yx} & I_y & -I_{yz} \\ -my_g & mx_g & 0 & -I_{zx} & -I_{zy} & I_z \end{bmatrix} \tag{3}$$

$$M_{RB}^{CG} = \begin{bmatrix} 52.000 & 0 & 0 & 0 & 0 & 0 \\ 0 & 52.000 & 0 & 0 & 0 & 0 \\ 0 & 0 & 52.000 & 0 & 0 & 0 \\ 0 & 0 & 0 & 0.404 & 0 & -0.057 \\ 0 & 0 & 0 & 0 & 8.930 & 0 \\ 0 & 0 & 0 & -0.057 & 0 & 8.922 \end{bmatrix}$$

Despite knowing that the body is not symmetric when using equation 2 and under the previously assumed conditions, we can observe in the main diagonal that the body has different moments of inertia for each axis (roll, pitch, yaw) 0.4040, 8.9300, 8.9220 respectively. Also, there is no coupling-effects between the translational DOF, this means that the translation in one axis is not affected by the translation in another axis of the sparus. On the other hand, there is a small coupling effect between roll and yaw. -0.0570 indicates that a rotation in roll (x-axis) generates a torque in yaw (z-axis), the negative value indicates that a torque generated by roll will be opposite to the movement in yaw and vice versa.

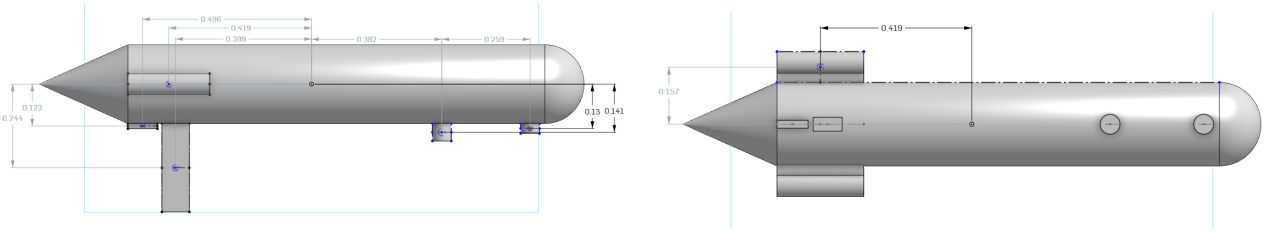

(a) Sparus II UV original CAD model (b) Sparus II UV simplified CAD model

Figure 6: Sparus II 3D models

In addition, by using a similar procedure as before, by isolating each part of the Sparu and by translating the center of mass of each part to the center of gravity of the AUV using CAD software, we can make an independent and comparative analysis of the effect of each mass matrix on the dynamics of the vehicle.

3.1 Mass matrix of main body, about CG.

$$M_{MB}^{CG} = \begin{bmatrix} 49.967 & 0 & 0 & 0 & 0 & 0 \\ 0 & 49.967 & 0 & 0 & 0 & 0 \\ 0 & 0 & 49.967 & 0 & 0 & 0 \\ 0 & 0 & 0 & 0.318 & 0 & 0 \\ 0 & 0 & 0 & 0 & 8.514 & 0 \\ 0 & 0 & 0 & 0 & 0 & 8.514 \end{bmatrix}$$

This mass matrix represents a rigid body with symmetric mass distribution about the translational degrees of freedom, and different moments of inertia for the rotational degrees of freedom, with no coupling or minimal effects between the degrees of freedom.

3.2 Mass matrix of Modem 1, about CG.

$$M_{M1}^{CG} = \begin{bmatrix} 0.060 & 0 & 0 & 0 & -0.008 & 0 \\ 0 & 0.060 & 0 & 0.008 & 0 & 0.039 \\ 0 & 0 & 0.060 & 0 & -0.039 & 0 \\ 0 & 0.008 & 0 & 0.001 & 0 & 0.005 \\ -0.008 & 0 & -0.039 & 0 & 0.026 & 0 \\ 0 & 0.039 & 0 & 0.005 & 0 & 0.025 \end{bmatrix}$$

For the first modem, we see the appearance of coupling-terms, which indicate that rotation in one axis will generate a torque in another; however, the effect is minimal. We can see that a rotation in roll will cause movement in the y direction and also a rotation in z. On the other hand, a rotation in yaw will cause a negative movement in the x direction and in the z direction. While a rotation in z will cause a positive movement in the y direction and a positive rotation in x.

3.3 Mass matrix of Modem 2/USBL, about CG.

$$M_{M2}^{CG} = \begin{bmatrix} 0.105 & 0 & 0 & 0 & -0.015 & 0 \\ 0 & 0.105 & 0 & 0.015 & 0 & 0.040 \\ 0 & 0 & 0.105 & 0 & -0.040 & 0 \\ 0 & 0.015 & 0 & 0.002 & 0 & 0.006 \\ -0.015 & 0 & -0.040 & 0 & 0.017 & 0 \\ 0 & 0.040 & 0 & 0.006 & 0 & 0.015 \end{bmatrix}$$

Because Modem 2 is also a cylinder like Modem 1, the mass matrix for Modem 2 has the same distribution, however, since it is larger, a slightly larger effect is evident.

3.4 Mass matrix of Antenna 1(Wifi/GPS/Flasher), about CG.

$$M_{A1}^{CG} = \begin{bmatrix} 0.680 & 0 & 0 & 0 & -0.166 & 0 \\ 0 & 0.680 & 0 & 0.166 & 0 & -0.271 \\ 0 & 0 & 0.680 & 0 & 0.271 & 0 \\ 0 & 0.166 & 0 & 0.044 & 0 & -0.066 \\ -0.166 & 0 & 0.271 & 0 & 0.153 & 0 \\ 0 & -0.271 & 0 & -0.066 & 0 & 0.109 \end{bmatrix}$$

On the other hand, we see that the effect of the mass matrix of Antenna 1 is much greater than the effects of the modems. Given its symmetry, we see how a force that causes movement in the x direction, can cause an anti-clockwise rotation in y. As well as a movement in y causes a clockwise rotation in x and an anti-clockwise rotation in z. While movement in z causes a clockwise rotation in y.

Therefore, when there is a rotation in x, a positive displacement in y and an anti-clockwise rotation in z is presented. In y, there is a force that causes a negative movement in x, a positive movement in z. While a moment in z causes an anti-clockwise rotation in y and a negative displacement in x.

3.5 Mass matrix of Antenna 2(Charging port/Gigabit Ethernet), about CG.

$$M_{A2}^{CG} = \begin{bmatrix} 0.025 & 0 & 0 & 0 & -0.003 & 0 \\ 0 & 0.025 & 0 & 0.003 & 0 & -0.012 \\ 0 & 0 & 0.025 & 0 & 0.012 & 0 \\ 0 & 0.003 & 0 & 0 & 0 & -0.001 \\ -0.003 & 0 & 0.012 & 0 & 0.006 & 0 \\ 0 & -0.012 & 0 & -0.001 & 0 & 0.006 \end{bmatrix}$$

Given that antenna 2 is a rectangular prism like antenna 1, its effects on the mass matrix are similar; however, given its size, its contribution to the mass is so small that even its coefficient m_{44} is very close to 0. So the mass matrix contributed by that object could be neglected.

3.6 Mass matrix of right thruster, about CG.

$$M_{RT}^{CG} = \begin{bmatrix} 0.770 & 0 & 0 & 0 & 0 & 0.121 \\ 0 & 0.770 & 0 & 0 & 0 & -0.323 \\ 0 & 0 & 0.770 & -0.121 & 0.323 & 0 \\ 0 & 0 & -0.121 & 0.020 & -0.052 & 0 \\ 0 & 0 & 0.323 & -0.052 & 0.139 & 0 \\ 0.121 & -0.323 & 0 & 0 & 0 & 0.159 \end{bmatrix}$$

For the right thruster we have that a movement in x can cause a clockwise rotation in z, while a movement in y can cause a negative rotation in z, on the other hand a force applied in z can cause a counter-clockwise rotation in x and a clockwise rotation in y.

In addition to this, a rotation at x has the potential to cause a negative movement at x and a counterclockwise rotation at y. While a rotation in y can cause a positive movement in z and a counterclockwise rotation in x. On the other hand, a rotation in y has the potential to cause a positive movement in z and a counterclockwise rotation in x. A rotation in z, on the other hand, can cause a positive movement in the x direction and a negative one in the y direction.

3.7 Mass matrix of left thruster, about CG.

$$M_{LT}^{CG} = \begin{bmatrix} 0.770 & 0 & 0 & 0 & 0 & -0.121 \\ 0 & 0.770 & 0 & 0 & 0 & -0.323 \\ 0 & 0 & 0.770 & 0.121 & 0.323 & 0 \\ 0 & 0 & 0.121 & 0.020 & 0.052 & 0 \\ 0 & 0 & 0.323 & 0.052 & 0.139 & 0 \\ -0.121 & -0.323 & 0 & 0 & 0 & 0.159 \end{bmatrix}$$

Because the thrusters are the same, the absolute values of the matrix are the same, however, the effects of the position in space of the left thruster on the Ssparrus, make some terms change their sign, for example now a displacement in x given by an applied force, will cause a counterclockwise rotation in z.

3.8 Comparison Mass matrices

Comparing the matrices, we can see that the main body plays has the largest effect on the overall sparrus mass matrix, followed by the thrusters and antenna 1. On the other hand, the contribution of antenna 2 is negligible. It is notable that the overall mass matrix has no cross-coupling terms between the transnational motions. Therefore, the motion in one direction will not affect the motion in another direction. However, there is a small effect between the forces that generate motion in x and a counterclockwise momentum in the z direction and vice versa.

4 Added mass computation

The hydrodynamic added mass is a virtual mass added to a system due to the displacement of fluid as an object accelerates or decelerates. Therefore, it is important to consider this added mass for accurate calculations of the system's dynamics, as the object and fluid cannot occupy the same physical space at the same time.

This added mass can significantly impact the dynamics of the AUV, altering the way the vehicle responds to forces and inputs. One method of calculating added mass is by utilizing slender body theory, which considers the vehicle's geometry and fluid properties, such as density and viscosity. This theory is assuming that the object is long and slender, meaning its length is significantly greater than its width and height.

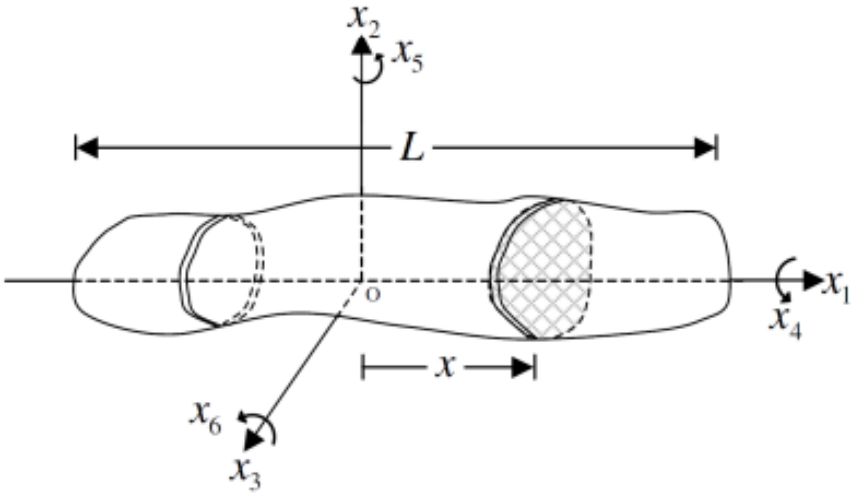

Figure 7: The added mass matrix based on slender body theorem.

4.1 Added mass matrix of main body, about CG.

Given the symmetry of the sparus the added mass matrix of the main body is given by:

$$Ma_{MB}^{CG} = \begin{pmatrix} \mathrm{ma}_{11} & 0 & 0 & 0 & 0 & 0 \\ 0 & \mathrm{ma}_{22} & 0 & 0 & 0 & \mathrm{ma}_{26} \\ 0 & 0 & \mathrm{ma}_{33} & 0 & \mathrm{ma}_{35} & 0 \\ 0 & 0 & 0 & \mathrm{ma}_{44} & 0 & 0 \\ 0 & 0 & \mathrm{ma}_{53} & 0 & \mathrm{ma}_{55} & 0 \\ 0 & \mathrm{ma}_{62} & 0 & 0 & 0 & \mathrm{ma}_{66} \end{pmatrix} \tag{4}$$

Dividing the main body into three intervals along its length:

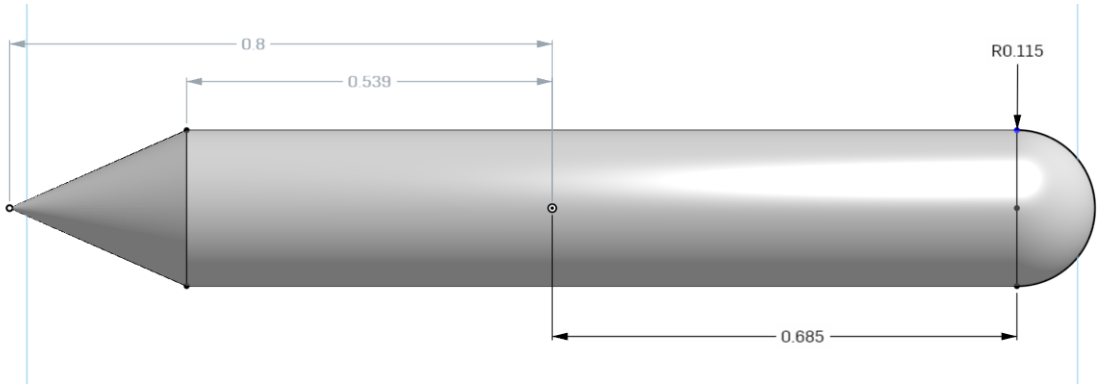

Figure 8: Slender body theory measurements for the main body.

$$a_{22} = \rho C_A A_r \tag{5}$$

$$A_r = \pi\ a^2\ , a = \text{radius of circle cross section} \tag{6}$$

$$Cone\ : a_1^2 = (0.4406 + (x + 0.8))^2 \tag{7}$$

$$Cylinder\ with\ two\ fins\ : a_2 = R; b = 0.2 \tag{8}$$

$$Cylinder\ : a_3^2 = R^2 \tag{9}$$

$$Half\ sphere\ : a_4^2 = R^2 - (x - 0.685)^2 \tag{10}$$

With the coefficients be:

$$m_{22} = \rho C_A \pi \left(\int_{-0.8}^{-0.539} a_1^2 \, \mathrm{dx} + \int_{-0.539}^{-0.299} a_2^2 \, \mathrm{dx} + \int_{-0.299}^{0.685} a_3^2 \, \mathrm{dx} + \int_{0.685}^{0.8} a_4^2 \, \mathrm{dx} \right) \tag{11}$$

$$m_{33} = \rho C_A \pi \left(\int_{-0.8}^{-0.539} a_1^2 \, \mathrm{dx} + \int_{-0.539}^{-0.299} b_2^2 \, \mathrm{dx} + \int_{-0.299}^{0.685} a_3^2 \, \mathrm{dx} + \int_{0.685}^{0.8} a_4^2 \, \mathrm{dx} \right) \tag{12}$$

$$m_{55} = \rho C_A \pi \left(\int_{-0.8}^{-0.539} x^2 a_1^2 \, \mathrm{dx} + \int_{-0.539}^{-0.299} x^2 b_2^2 \, \mathrm{dx} + \int_{-0.299}^{0.685} x^2 a_3^2 \, \mathrm{dx} + \int_{0.685}^{0.8} x^2 a_4^2 \, \mathrm{dx} \right) \tag{13}$$

$$m_{66} = \rho C_A \pi \left(\int_{-0.8}^{-0.539} x^2 a_1^2 \, \mathrm{dx} + \int_{-0.539}^{-0.299} x^2 a_2^2 \, \mathrm{dx} + \int_{-0.299}^{0.685} x^2 a_3^2 \, \mathrm{dx} + \int_{0.685}^{0.8} x^2 a_4^2 \, \mathrm{dx} \right) \tag{14}$$

$$m_{26} = \rho C_A \pi \left(\int_{-0.8}^{-0.539} x \, a_1^2 \, \mathrm{dx} + \int_{-0.539}^{-0.299} x \, a_2^2 \, \mathrm{dx} + \int_{-0.299}^{0.685} x \, a_3^2 \, \mathrm{dx} + \int_{0.685}^{0.8} x \, a_4^2 \, \mathrm{dx} \right) \tag{15}$$

$$m_{35} = -\rho C_A \pi \left(\int_{-0.8}^{-0.539} x \, a_1^2 \, \mathrm{dx} + \int_{-0.539}^{-0.299} x \, b_2^2 \, \mathrm{dx} + \int_{-0.299}^{0.685} x \, a_3^2 \, \mathrm{dx} + \int_{0.685}^{0.8} x \, a_4^2 \, \mathrm{dx} \right) \tag{16}$$

$$m_{53} = m_{35} \tag{17}$$

$$m_{26} = m_{62} \tag{18}$$

The two thrusters are often treated as fins in added mass calculations because when they are considered as separate bodies, the water flow between the thruster and the main body is not accurately accounted for. Therefore, it is more accurate to include them in the main body's added mass calculations.

The resulted added mass is given by:

$$Ma_{MB}^{CG} = \begin{bmatrix} 0 & 0 & 0 & 0 & 0 & 0 \\ 0 & 57.654 & 0 & 0 & 0 & 3.848 \\ 0 & 0 & 77.842 & 0 & 4.611 & 0 \\ 0 & 0 & 0 & 0 & 0 & 0 \\ 0 & 0 & 4.611 & 0 & 13.281 & 0 \\ 0 & 3.848 & 0 & 0 & 0 & 9.640 \end{bmatrix}$$

4.1.1 m_{44} Coefficient, main body added mass matrix.

For m_{44}, the added mass is not zero because when rotating around x-axis, the two thrusters which are considered as two fins displace water. We can calculate this value from the set of equations for added mass moment of inertia for a cylinder with two fins cross-section.

$$m_{44} = \frac{\rho \, a^4 \, (csc^4(\alpha) \, f(\alpha) - \pi^2)}{2 \, \pi} \, L_{fins}$$

where

$$b = 0.200$$

$$a = 0.115$$

$$L_{fins} = 0.240$$

$$\alpha = asin\left(\frac{2 \, a \, b}{a^2 + b^2}\right) \, \frac{180}{\pi}$$

$$\alpha = (\alpha + 60)\frac{\pi}{180}$$

As a result, we have:

$$m_{44} = 0.0199$$

By updating with m_{44} the added mass matrix for the main body, we got that:

$$Ma^{CG}_{MB} = \begin{bmatrix} 0 & 0 & 0 & 0 & 0 & 0 \\ 0 & 57.654 & 0 & 0 & 0 & 3.848 \\ 0 & 0 & 77.842 & 0 & 4.611 & 0 \\ 0 & 0 & 0 & 0.019 & 0 & 0 \\ 0 & 0 & 4.611 & 0 & 13.281 & 0 \\ 0 & 3.848 & 0 & 0 & 0 & 9.640 \end{bmatrix}$$

4.1.2 m_{11} Coefficient, for the main body added mass matrix.

One limitation of slender body theory is that it cannot estimate the added mass due to acceleration along the x-axis (m_{11}). To overcome this limitation, Lamb's k-factor for spheroid can be used to estimate this value. This method involves considering the main body as three spheroids to estimate m_{11}.

Knowing that the added mass using Lamb's k-factor is given by:

$$m_{df} = \frac{4}{3}\,\pi\,\rho\,a\,b^2 \tag{19}$$

$$e = \sqrt{(1 - \frac{b^2}{a^2})} \tag{20}$$

$$\alpha_0 = 2\frac{1-e^2}{e^3}\left(\frac{1}{2}ln\left(\frac{1+e}{1-e}\right) - e\right) \tag{21}$$

$$k_1 = \frac{\alpha_0}{2-\alpha_0} \tag{22}$$

$$m_{11} = k_1\,m_{df} \tag{23}$$

- For the Main body without Thrusters.

$$a = 0.8$$
$$b = 0.115$$

As a result, we have that:

$$m_{11} = 1.604$$

- For the Right Thruster.

$$a = 0.120$$
$$b = 0.310$$

As a result, we have m_{11} for the right thruster is:

$$m_{11} = 0.041$$

However, we must, transferred it to the center of the gravity using the *transformation matrix H*, defined by:

$$H(r^b_g) = \begin{bmatrix} I_{3\times3} & S^T(r^b_g) \\ 0_{3\times3} & I_{3\times3} \end{bmatrix} \tag{24}$$

with the vector r_g^b defined as:

$$r_g^b = \begin{bmatrix} -0.419 \\ 0.157 \\ 0 \end{bmatrix}$$

then:

$$Ma_{RT}^{CG} = H(r_g^b)^T \, Ma_{RT} \, H(r_g^b)$$

The resulted matrix is:

$$Ma_{RT}^{CG} = \begin{bmatrix} 0.041 & 0 & 0 & 0 & 0 & 0.006 \\ 0 & 0 & 0 & 0 & 0 & 0 \\ 0 & 0 & 0 & 0 & 0 & 0 \\ 0 & 0 & 0 & 0 & 0 & 0 \\ 0 & 0 & 0 & 0 & 0 & 0 \\ 0.006 & 0 & 0 & 0 & 0 & 0.001 \end{bmatrix}$$

It can be observed that when transforming from the center of the thruster to the center of the vehicle, there is a minimal value present in the cross-terms. This is due to the relative position of the thruster to the main body and the effect it has on the displacement of fluid and the added mass calculations.

- For the Left Thruster.

The calculation process is similar to that of the right thruster, but the values of m_{16} and m_{61} are negative due to the position of the left thruster.

$$Ma_{LT}^{CG} = \begin{bmatrix} 0.041 & 0 & 0 & 0 & 0 & -0.006 \\ 0 & 0 & 0 & 0 & 0 & 0 \\ 0 & 0 & 0 & 0 & 0 & 0 \\ 0 & 0 & 0 & 0 & 0 & 0 \\ 0 & 0 & 0 & 0 & 0 & 0 \\ -0.006 & 0 & 0 & 0 & 0 & 0.001 \end{bmatrix}$$

By updating with, m_{11} we finally got that the added mass matrix for the main body is given by:

$$Ma_{MB}^{CG} = \begin{bmatrix} 1.604 & 0 & 0 & 0 & 0 & 0 \\ 0 & 57.654 & 0 & 0 & 0 & 3.848 \\ 0 & 0 & 77.842 & 0 & 4.611 & 0 \\ 0 & 0 & 0 & 0.019 & 0 & 0 \\ 0 & 0 & 4.611 & 0 & 13.281 & 0 \\ 0 & 3.848 & 0 & 0 & 0 & 9.640 \end{bmatrix}$$

4.2 Added mass matrix of Antenna 1, about CG.

This particular section of the AUV will be modeled as a cuboid with a square cross-section, which is long in the z-axis. Therefore, when using slender body theory, integration must be performed along the z-axis. However, the ratio of **length (L)** to **width/height (b/a)** is less than **10**, which means that using slender body theory will not provide accurate estimates of the added mass for this section.

The added mass of the Antenna 1 is given by:

$$Ma_{A1} = \begin{bmatrix} 0.497 & 0 & 0 & 0 & 0 & 0 \\ 0 & 1.764 & 0 & 0 & 0 & 0 \\ 0 & 0 & 0 & 0 & 0 & 0 \\ 0 & 0 & 0 & 0.010 & 0 & 0 \\ 0 & 0 & 0 & 0 & 0.003 & 0 \\ 0 & 0 & 0 & 0 & 0 & 0.195 \end{bmatrix}$$

The *transformation H matrix* is used to transform this added mass matrix to the center of the vehicle.

$$Ma_{A1}^{CG} = \begin{bmatrix} 0.497 & 0 & 0 & 0 & -0.121 & 0 \\ 0 & 1.764 & 0 & 0.430 & 0 & -0.704 \\ 0 & 0 & 0 & 0 & 0 & 0 \\ 0 & 0.430 & 0 & 0.115 & 0 & -0.172 \\ -0.121 & 0 & 0 & 0 & 0.032 & 0 \\ 0 & -0.704 & 0 & -0.172 & 0 & 0.475 \end{bmatrix}$$

4.3 Added mass matrix of Modem 1, about CG.

When using the slender body theory to calculate the added mass, the modem 1 is considered as a cylinder. The ratio of the length to the diameter is used to estimate the added mass coefficient (C_A) and calculate the added mass matrix at the center of the sensor. The calculated added mass matrix is then transferred to the center of the vehicle using the transformation matrix (H). This results in an estimation of the added mass of the sensor at the center of the vehicle.

$$Ma_{M1}^{CG} = \begin{bmatrix} 0.075 & 0 & 0 & 0 & -0.011 & 0 \\ 0 & 0.075 & 0 & 0.011 & 0 & 0.029 \\ 0 & 0 & 0 & 0 & 0 & 0 \\ 0 & 0.011 & 0 & 0.001 & 0 & 0.004 \\ -0.011 & 0 & 0 & 0 & 0.001 & 0 \\ 0 & 0.029 & 0 & 0.004 & 0 & 0.011 \end{bmatrix}$$

4.4 Added mass matrix of Modem 2, about CG.

The same calculation process used for sensor one is applied to sensor 2, which includes using the ratio of length to diameter to estimate the added mass coefficient (C_A) and calculating the added mass matrix at the center of the sensor. Then the added mass matrix is transferred to the center of the vehicle using the transformation matrix (H). This results in an estimation of the added mass of sensor 2 at the center of the vehicle.

$$Ma_{M2}^{CG} = \begin{bmatrix} 0.043 & 0 & 0 & 0 & -0.006 & 0 \\ 0 & 0.043 & 0 & 0.006 & 0 & 0.027 \\ 0 & 0 & 0 & 0 & 0 & 0 \\ 0 & 0.006 & 0 & 0.001 & 0 & 0.004 \\ -0.006 & 0 & 0 & 0 & 0.001 & 0 \\ 0 & 0.027 & 0 & 0.004 & 0 & 0.018 \end{bmatrix}$$

4.5 Total Added mass matrix, about CG.

AS a result, we have that the total added mass matrix is given by:

$$Ma_{RB}^{CG} = Ma_{MB}^{CG} + Ma_{RT}^{CG} + Ma_{LT}^{CG} + Ma_{A1}^{CG} + Ma_{M1}^{CG} + Ma_{M2}^{CG} \tag{25}$$

Therefore, we have that:

$$Ma_{RB}^{CG} = \begin{bmatrix} 2.302 & 0 & 0 & 0 & -0.137 & 0 \\ 0 & 59.536 & 0 & 0.446 & 0 & 3.200 \\ 0 & 0 & 77.842 & 0 & 4.611 & 0 \\ 0 & 0.446 & 0 & 0.137 & 0 & -0.164 \\ -0.137 & 0 & 4.611 & 0 & 13.316 & 0 \\ 0 & 3.200 & 0 & -0.164 & 0 & 10.146 \end{bmatrix}$$

4.6 Comparisons between added mass matrices.

The diagonal elements of the added mass matrix indicate that the vehicle experiences the most added mass in the z and y directions, while the added mass in the x-direction is relatively small. This is due to the thrusters displacing more water when moving in the z-direction and the symmetry of the vehicle around the x-axis, resulting in a small added mass due to rotation along the x-axis. However, rotation along the z and y directions results in a higher added mass due to a larger amount of water being displaced.

The off-diagonal terms in the matrix, though small in comparison to the diagonal terms, can have a significant effect on the dynamics of the vehicle. These terms exist due to the interaction between the motion of the vehicle in different directions. For example, as the vehicle moves in the x-direction, it also experiences added mass in the y and z directions. The values for off-diagonal terms can be positive or negative, representing the correlation between different directions.

From the added mass matrices, it can be seen that the impact of the antenna and sensors on the overall added mass of the vehicle is relatively small compared to the added mass calculated for the main body. The antenna has a value of 0.5 and 1.7 kg in the x and y directions respectively, while the sensors have minimal values that can be ignored.

5 Drag matrix computation

Calculating the drag matrices for the Sparrus involves several steps:

1. Splitting the body of the vehicle into main parts: main body, thrusters, antenna and sensors.
2. These parts have a shape that the drag coefficient can be estimated. The drag coefficients can be calculated using empirical equations based on the vehicle's geometry, the fluid properties, and the Reynolds number. We considered turbulent flow.
3. Calculating the projected surface area in every direction (x, y and z)
4. Compute the diagonal drag matrix K_{qi}^{bi} for each body.

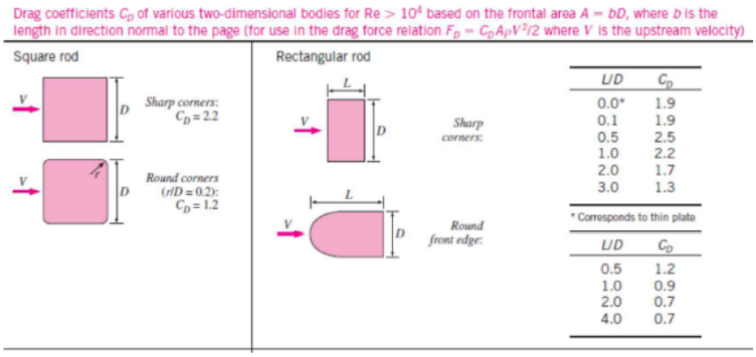

Figure 9: 2D Drag coefficient table.

5.1 Main Body Drag Matrix

We can estimate the effect of main body shape is similar to a sphere when moving in water as it has a hemisphere at the front and cone at the back which we considered the cone as another hemisphere. We estimated the following drag coefficients:

- 3D drag coefficient in x-direction: $C_{D11} = 0.2$.
- the 2D drag coefficient along the length in the y direction and z direction: : $C_{D22} = C_{D33} = 0.3$ as the cross-section is a circle, and we assume that the radius is constant.

We computed the projected surface area based on the dimension of the cylinder and obtained the following matrix.

$$D_{MB} = \begin{bmatrix} 4.155 & 0 & 0 & 0 & 0 & 0 \\ 0 & 55.200 & 0 & 0 & 0 & 0 \\ 0 & 0 & 55.200 & 0 & 0 & 0 \\ 0 & 0 & 0 & 0 & 0 & 0 \\ 0 & 0 & 0 & 0 & 7.066 & 0 \\ 0 & 0 & 0 & 0 & 0 & 7.066 \end{bmatrix}$$

The values in the diagonal show that the drag force is higher in the y and z-direction than in the x-direction. The values in the diagonal indicate that the drag force acts differently in each degree of freedom. However, there is no drag forces related to the rotation in the x-axis, probably because the drag force for this DOF is negligible. Nevertheless, in the case of thrusters, the contribution of the Matrix drag regarding the main body is significantly smaller.

5.2 Right and Left Drag Matrix

The diagonal drag matrix is the same for both thrusters. The thruster takes the shape of a hemisphere at one end, and the other end is flat. So, we considered it a hemisphere mowing in water. It produces the same drag effect. We estimated the following drag coefficients:

- 3D drag coefficient in x-direction: $C_{D11} = 0.4$.
- The 2D drag coefficient along the length in the y direction and z direction: : $C_{D22} = C_{D33} = 0.3$as the cross-section is a circle, and we assume that the radius is constant.

We computed the projected surface area based on the dimension of the cylinder and obtained the following matrix:

$$D_{LRT} = \begin{bmatrix} 0.604 & 0 & 0 & 0 & 0 & 0 \\ 0 & 8.280 & 0 & 0 & 0 & 0 \\ 0 & 0 & 8.280 & 0 & 0 & 0 \\ 0 & 0 & 0 & 0 & 0 & 0 \\ 0 & 0 & 0 & 0 & 0.004 & 0 \\ 0 & 0 & 0 & 0 & 0 & 0.004 \end{bmatrix}$$

Similar to the previous case, the values in the diagonal show that the drag force is higher in the y and z-direction than in the x-direction. The values in the diagonal indicate that the drag force acts differently in each degree of freedom. However, there is no drag forces related to the rotation in the x-axis, probably because the drag force for this DOF is negligible.

5.3 Antenna 1 Drag Matrix

The antenna takes the shape of the cuboid with rounded edges. We estimated the following drag coefficients based on the height ($a = 0.08m$), width ($b = 0.038$) and length ($L = 0.258$):

- 3D drag coefficient in z-direction: $C_{D33} = 1.05$. it is estimated in z because the antenna is long in that direction.
- The projected surface of the antenna in y-axis is a rounded edge rectangle and the ratio of $a/b = 2.1$ and $b/a = 0.47$ so we selected the 2D drag coefficient along the length in the x direction and y direction: $C_{D11} = 0.7$ and $C_{D22} = 1.2$.

The diagonal drag matrix for the antenna is:

$$D_{A1} = \begin{bmatrix} 3.431 & 0 & 0 & 0 & 0 & 0 \\ 0 & 12.384 & 0 & 0 & 0 & 0 \\ 0 & 0 & 1.596 & 0 & 0 & 0 \\ 0 & 0 & 0 & 0.003 & 0 & 0 \\ 0 & 0 & 0 & 0 & 0.004 & 0 \\ 0 & 0 & 0 & 0 & 0 & 0 \end{bmatrix}$$

The values on the diagonal show that the drag force is higher in the x, y and z-direction but specially in y-direction. On the other hand, the drag forces on the rotational DOF are negligible.

5.4 Thrusters matrix

A thruster mapping matrix is obtained to relate forces and moments on the vehicle to the thrust forces of the three thrusters. Given the position of each thruster, we can calculate the thrust forces and moments represented by the following equation:

$$U_b = E^b \, F_T^b = E_{6*3}^b \begin{bmatrix} F_{T1}^b \\ F_{T2}^b \\ F_{T3}^b \end{bmatrix} \tag{26}$$

Where F_T^b is the force of thruster (or motor) in Body-fixed frame. We can obtain the Thruster mapping matrix E^b given the position of the thrusters.

$$E^b = \begin{bmatrix} 0 & 1 & 1 \\ 0 & 0 & 0 \\ 1 & 0 & 0 \\ 0 & 0 & 0 \\ 0 & 0 & 0 \\ 0 & -0.17 & 0.17 \end{bmatrix}$$

5.5 Comparison between drag matrices

When comparing the drag matrices, we can see that a large portion of the forces caused by the movement of the Sparus are generated by the main body. Especially in the y and z directions. While the drag in the rotational DOF is practically zero.

6 Simluation of the model

After updating the parameters.m file with the matrices calculated, you can use the Sparus simulator to simulate the dynamics of the vehicle under different conditions. The simulation will consider the added mass and drag matrices for each body, as well as the global mass matrix. This will provide a more accurate representation of the vehicle's behavior in the water.

We updated *rov_model.m* the function to calculate the Coriolis forces and friction forces.

1. Compute diagonal drag matrix $K_{q,i}^{bi}$.Except the main body, the moment coefficients are neglected.

2. Compute the speed at Buoyancy center of each body from the speed measure point (DVL position):

$$V_{b_i/n}^b = H\left(\overrightarrow{C_{DVL}b_i}\right) V_{C_{DVL/n}}^b$$

3. The global drag force of a body expressed on its buoyancy center b_i is:

$$\tau_{b_{i,i}}^b = K_{q,i}^{b_i} * \left|V_{b_i/n}^b\right| * \left|V_{b_i/n}^b\right|$$

We did the simulation for the whole Sparus vehicle including thrusters, antenna and sensors.

6.1 Simple model validation

For the first validation, the only thing that was done was to set the thrusters at 100%.

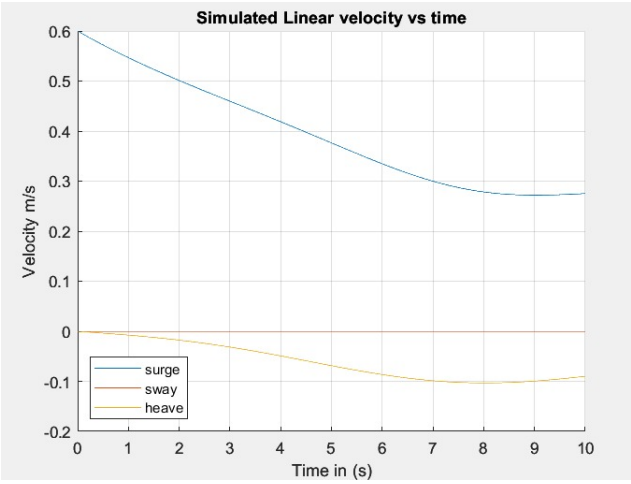

(a) Simulated Position vs time

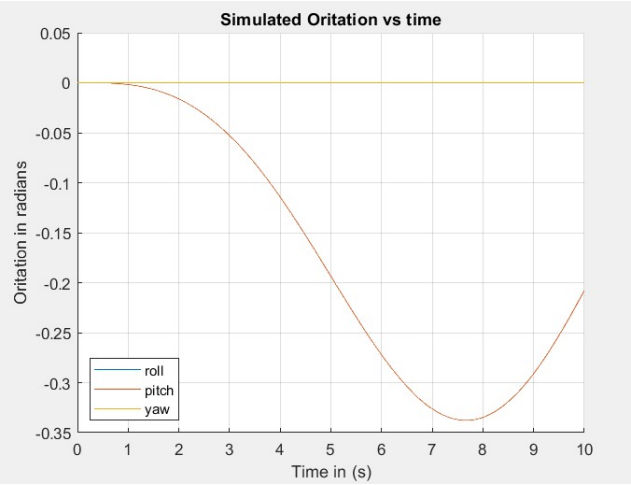

(b) Simulated Orientation vs time

Figure 10: Position and orientation over the time

We can see how over time the Sparrus begins to move in the positive direction of x (surge), at the same time as it begins to ascend to the surface, which in the case of autonomous underwater vehicles is the negative direction of the z-axis. While pitching in the clockwise direction with an incremental trend.

6.2 Simple model applying a linear acceleration

Because the Thruster were turned off, the linear acceleration result are not necessary.

6.3 Simple model applying a constant speed

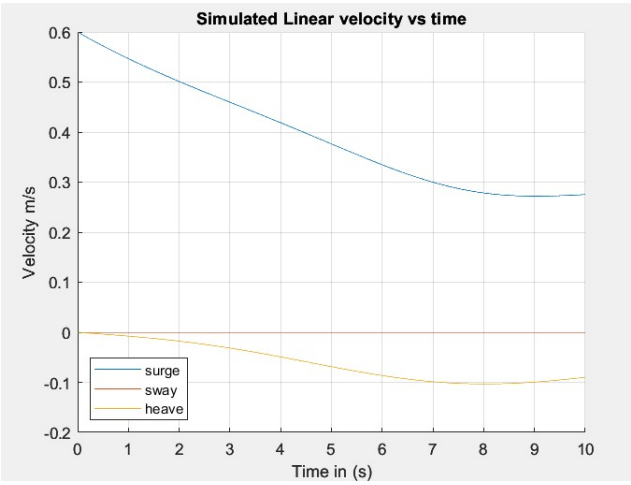

(a) Simulated constant velocity vs time

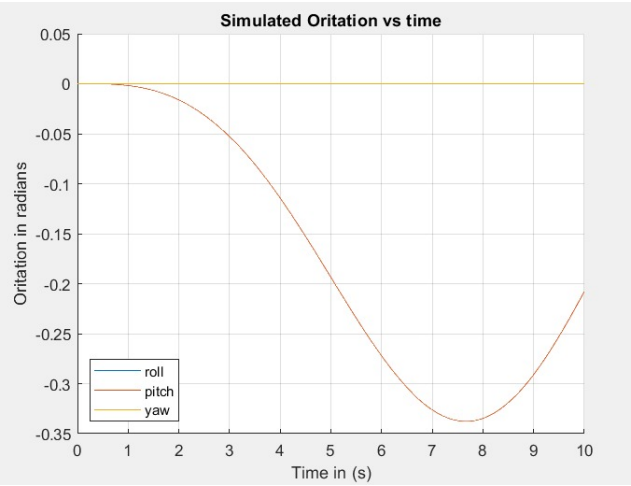

(b) Simulated Orientation vs time

Figure 11: Simultaed orientation at constant speed vs time

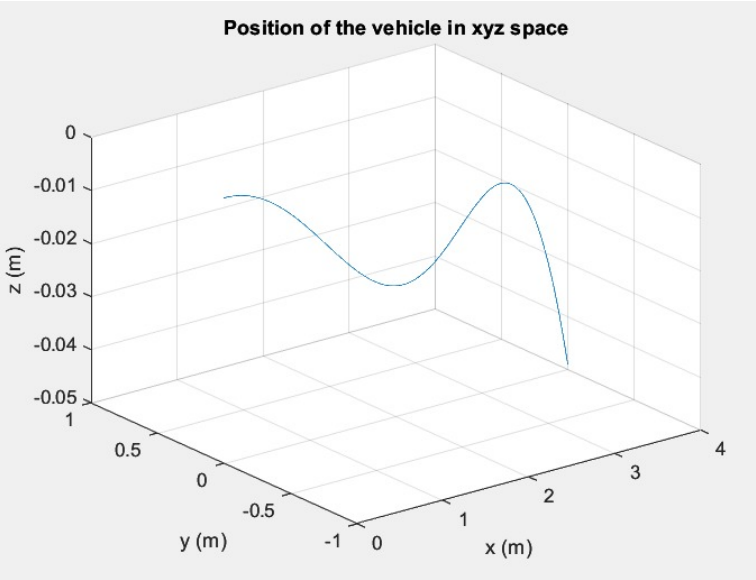

Figure 12: 3D position at constant speed.

We can see how as the velocity decreases in the x and z axes, the vehicle starts to ascend due to the buoyancy for which it was designed, while it slightly pitches and moves in the surge direction.

7 Conclusions

In conlusion, this report aimed to understand the theory behind the accurate mathematical modeling of an AUV. The Sparus II AUV was analyzed by calculating various elements for rigid body dynamics, such as the system inertia matrix and damping equation, and simulating their effects on the vehicle's movement. It was found that symmetrical components had a lower added mass and less cross-coupling effects, making them more favorable for control purposes. Additionally, the drag and added mass matrices were calculated and their effects on the dynamics of the system were studied through simulations. It was concluded that the drag and added mass are important factors that should be considered in the design of the vehicle, and that these calculations are only valid for specific operating conditions and may change with changes in the operating environment.

8 Bibliography

1. RICHIER Marthieu, Introduction to Underwater Robotics, Modelling and Control, MIR master's Degree, 2022.

2. FOSSEN I. Thor, Guidance and control of Ocean Vehicles, University of Trondheim, Jhon Wiley and Sons, Norway,1998.

3. FOSSEN I. Thor, Handbook of marine craft hydrodynamics and control, Norwegian University of Science and Technology, John Wiley and Sons, Ltd, Norway,2011.